DOI: 10.1002/ejic.200801187

Cobalt and Silver Complexes of Terdentate Pyrazine-Based Amide Ligands and Assembly of Monocobalt Building Blocks through a Silver Connector

Ryan M. Hellyer,[a] David S. Larsen,[a] and Sally Brooker*[a]

Keywords: Pyrazine / Cobalt / Silver / Mixed-metal complexes / Electrochemistry / Amides

Two terdentate pyrazine-based amide ligands have been prepared from methyl pyrazine-2-carboxylate and 2-(aminomethyl)pyridine ($H\mathbf{L^{1M}}$) or 2-(2-aminoethyl)pyridine ($H\mathbf{L^{1E}}$) in order to probe the potential of the "spare" nitrogen atom "out the back" of the pyrazine ring to coordinate to a different metal ion and thereby act as a linker between complexes. Two inert cobalt(III) complexes, $[Co^{III}(\mathbf{L^{1M}})_2](BF_4)\cdot\frac{1}{4}H_2O$ and $[Co^{III}(\mathbf{L^{1E}})_2](BF_4)\cdot\frac{1}{2}H_2O$, have been prepared as building blocks and the silver(I) coordination of the ligands also probed, forming $\{[Ag^{I}(H\mathbf{L^{1M}})]BF_4\}_\infty$ and $[Ag^{I}_2(H\mathbf{L^{1LE}})_2](BF_4)_2$. The $[Co^{III}(\mathbf{L^{1E}})_2](BF_4)$ building block has been successfully connected to a second such complex by coordination of silver(I) to a "spare" pyrazine nitrogen atom on each complex, resulting in $[\{Co^{III}(\mathbf{L^{1E}})_2\}_2Ag^{I}](BF_4)(NO_3)_2$. All five complexes have been structurally characterised. Mass spectra and cyclic voltammetry studies on "aged" (kept in solution in air for 2 d) samples clearly showed that the cobalt complex of the methylene-linked ligand was prone to slow ligand oxidation, forming $[Co^{III}(\mathbf{L^{1Mox}})(\mathbf{L^{1M}})](BF_4)$ and $[Co^{III}(\mathbf{L^{1Mox}})_2](BF_4)$. Fresh samples of $[Co^{III}(\mathbf{L^{1M}})_2](BF_4)\cdot\frac{1}{4}H_2O$ and $[Co^{III}(\mathbf{L^{1E}})_2](BF_4)\cdot\frac{1}{2}H_2O$ undergo a chemically reversible one-electron reduction in dry acetonitrile, at –0.71 and –0.48 V vs. 0.01 M $AgNO_3$/Ag, respectively, consistent with the methylene-linked ligand being better able to stabilise the higher oxidation state of cobalt than the ethylene-linked ligand.

Introduction

The self-assembly of molecular grids, especially tetrametallic [2×2] grids, has been studied extensively over the past decade.[1] Such complexes have interesting and potentially useful magnetic and electronic properties. For example, the Lehn group has described the first tetrametallic spin-crossover complex[2] and has also reported the highest number of well-resolved and reversible one-electron reductions for a molecular compound;[3] in both cases the complexes concerned were tetrametallic [2×2] grids. Such complexes are of great interest not only for reasons of fundamental science but also because of their potential development for use in future high-density storage devices.[1–3]

The bis(terdentate) pyrazine-based diamide ligands $H_2\mathbf{L^{2M}}$ and $H_2\mathbf{L^{2E}}$ (Figure 1) have been used to produce tetrametallic [2×2] grids when complexed with octahedral metal(II) ions in a 1:1 stoichiometry.[5] In order to access larger arrays of metal ions, rather than constructing ever larger ligands (i.e. with more binding pockets per ligand strand), our approach is to instead connect the [2×2] grids together in a manner similar to that proposed and demonstrated by Lehn and co-workers,[6] i.e. by subsequent metal-ion bridging of "spare" donor atoms "out the back" of the tetrametallic [2×2] grid. In parallel with developing the "all-pyrazine" ligand analogues of $H_2\mathbf{L^{2M}}$ and $H_2\mathbf{L^{2E}}$ for this purpose, a task that involves significant synthetic challenges,[7] a test system has been prepared, which is the subject of this paper.

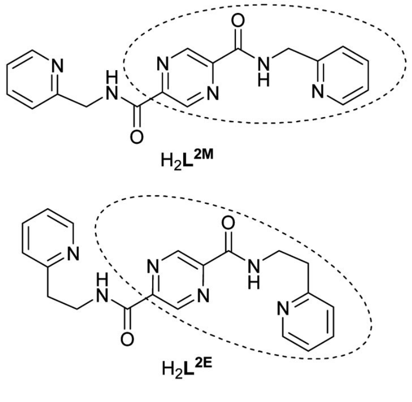

Figure 1. Pyrazine diamide ligands $H_2\mathbf{L^{2M}}$ and $H_2\mathbf{L^{2E}}$ used, by us and others, in previous work.[4,5] Dotted ellipses indicate the portion of these ligands that corresponds to $H\mathbf{L^{1M}}$ and $H\mathbf{L^{1E}}$ (top and bottom, respectively), the ligands used in this work (see also Scheme 1).

$H\mathbf{L^{1M}}$ and $H\mathbf{L^{1E}}$, which are very similar to $H_2\mathbf{L^{2M}}$ and $H_2\mathbf{L^{2E}}$ but with only one alkylpyridine arm, have been prepared (Figure 1, Scheme 1). On binding two of these terdentate ligands to an octahedral metal ion, one of the

---

[a] Department of Chemistry and MacDiarmid Institute for Advanced Materials and Nanotechnology, University of Otago,
Dunedin, New Zealand
Fax: +64-3-4797906
E-mail: sbrooker@chemistry.otago.ac.nz

Supporting information for this article is available on the WWW under http://www.eurjic.org or from the author.

pyrazine nitrogen atoms out the back of each ligand will be spare. Subsequent coordination of these spare nitrogen donors in the "building block" complex to another metal ion will allow us to test whether these complexes can be linked together. Whilst cobalt(III) is not our usual first row metal ion of choice as it is diamagnetic, in this case it was chosen for the building block complexes as the +3 charge should challenge the ability of the spare pyrazine nitrogen atom with regard to binding to the linker metal ion (the [2×2] grid complexes of $H_2\mathbf{L^{2M}}$ and $H_2\mathbf{L^{2E}}$ prepared to date feature +2 oxidation states; so the all-pyrazine analogues of these complexes should be able to more readily bind to the linker-metal ion). Silver(I) was chosen as the linker-metal ion as it is labile and frequently forms approximately linear bonds. For completeness, the silver(I) coordination chemistry of these two ligands was also probed. In this paper, we report the results of these investigations, including the stepwise synthesis of the two ligands, the synthesis and structures of five cobalt and silver complexes, and a careful and illuminating electrochemical study of the cobalt(III) complexes.

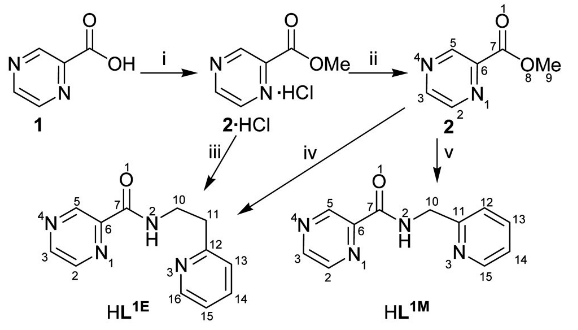

Scheme 1. Synthesis of the ligands used in this work. (i) $SOCl_2$/MeOH, (ii) K_2CO_3/CH_2Cl_2, (iii) 2 equiv. 2-(2-aminoethyl)pyridine, (iv) 1 equiv. 2-(2-aminoethyl)pyridine, (v) 1 equiv. 2-(aminomethyl)pyridine.

A SciFinder Scholar[8] substructure search (search fragment shown in Figure 2 with X = N) revealed that, with the exception of the handful of complexes of $H_2\mathbf{L^{2M}}$ and $H_2\mathbf{L^{2E}}$ that we and others have reported,[4,5] *only three papers* report metal complexes featuring a *pyrazine*-amide-linker-pyridine motif. All three are communications, published in 2007 or 2008, and appeared after our own research program was well underway. Firstly, Hong and co-workers published two communications in 2007 describing the preparation and use of $[\mathrm{Fe^{III}}(\mathbf{L^3})(\mathrm{CN})_3]^-$ as building block (Figure 2) for $\mathrm{Fe^{III}}$–CN–$\mathrm{Mn^{III}}$ ferrimagnetic chains, one of which exhibits a metamagnetic transition.[9] Then, in 2008, Hubin and co-workers[10] communicated the structure of a trimetallic mixed-valent complex of $\mathbf{HL^{1M}}$ (Figure 1), $[\{\mathrm{Co^{III}}(\mathbf{L^{1M}})_2\}_2\text{-}\{\mathrm{Co^{II}}(H_2O)_2Cl_2\}]Cl_2$. They did not isolate the monomeric species $[\mathrm{Co^{III}}(\mathbf{L^{1M}})_2]$X.

In contrast, the analogous *pyridine*-amide-linker-pyridine motif has been far more extensively studied. A SciFinder Scholar[8] substructure search for the same fragment but with X = C (Figure 2) revealed over 100 papers concerning such complexes. Of these, the handful of cobalt complexes, of ligands such as those shown in Figure 2, is most relevant to this work.[11–14] No silver complexes were found.

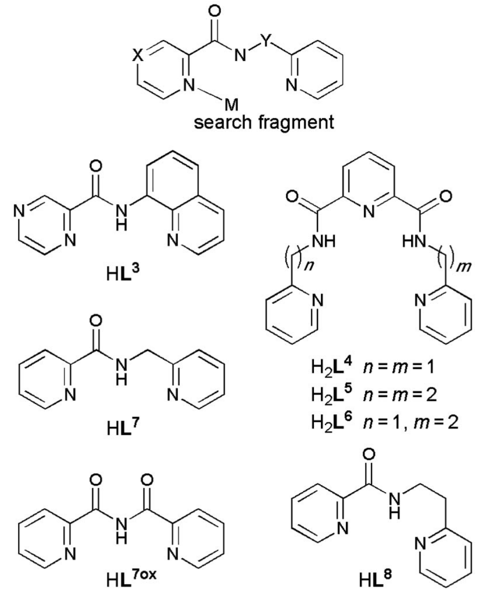

Figure 2. SciFinder Scholar search fragment (X = C or N, Y = one- or two-carbon atom linker); "hits" included complexes of the ligands, $\mathbf{HL^3}$, $H_2\mathbf{L^4}$, $H_2\mathbf{L^5}$, $H_2\mathbf{L^6}$, $\mathbf{HL^7}$, $\mathbf{HL^{7ox}}$ and $\mathbf{HL^8}$ (shown here), as well as complexes of the ligands shown in Figure 1.

The $\mathbf{HL^7}$ and $\mathbf{HL^8}$ ligands (Figure 2) are the pyridine-based analogues of our pyrazine-based ligands $\mathbf{HL^{1M}}$ and $\mathbf{HL^{1E}}$ (Figure 1, Scheme 1). Nonoyama and Yamasaki reported the synthesis, from cobalt(II) reagents in air, of $[\mathrm{Co^{III}}(\mathbf{L^7})_2]^+$, $[\mathrm{Co^{III}}(\mathbf{L^8})_2]^+$ and $\mathrm{Co^{II}}(\mathbf{HL^8})_2X_2$. They found that a base, NaOH, had to be used to deprotonate $\mathbf{HL^8}$, whereas $\mathbf{HL^7}$ spontaneously deprotonated in the presence of the metal ion.[11] Mascharak and co-workers, in the course of studies aimed at modelling the activation of bleomycins (glycopeptide antibiotics that cleave DNA), subsequently found that, whereas the ligand $(\mathbf{L^7})^-$ is stable in air, when ligated to $\mathrm{Fe^{III}}$ or $\mathrm{Co^{III}}$ centers it is oxidised by air to $(\mathbf{L^{7ox}})^-$ (Figure 2).[14] They proposed that the likely driving force for the formation of the oxidised ligand is that conversion of the methylene group to a carbonyl group is energetically favourable due to the resulting conjugation with the aromatic ring. Interestingly, they were unable to oxidise the ligand by adding ferrocinium tetrafluoroborate to the complexation reaction. However, simply stirring the reaction solution in air gave $[\mathrm{Co^{III}}(\mathbf{L^{7ox}})_2]ClO_4$. The determination of the single-crystal structure, but no electrochemical study, was reported.[14] It should be noted that the imide, $\mathbf{HL^{7ox}}$, has also been prepared by other routes, for example by copper(II)-catalysed hydrolysis of 1,3,5-tris(2-pyridyl)triazine followed by EDTA extraction (to remove the copper ions)[15] and by deliberate organic synthesis from pyridine-2-carboxylic acid, by reaction with PCl_5 followed by liquid NH_3.[16] Simultaneous with the work of Mascharak and co-workers, Kajiwara and co-workers reported the preparation of $[\mathrm{Co^{III}}(\mathbf{L^{7ox}})_2](ClO_4)$ from preformed $\mathbf{HL^{7ox}}$ and that it undergoes two reversible reductions in MeCN, at –0.28 and –1.66 V vs. SSCE (ca. –0.22 and –1.60 V vs. 0.01 M $\mathrm{AgNO_3/Ag}$[17]), processes that they assumed to be metal-centred.[13]

Results and Discussion

Ligand Synthesis

N-(2-Pyridylmethyl)pyrazine-2-carboxamide ($\mathrm{H}\mathbf{L^{1M}}$) and *N*-[2-(2-pyridyl)ethyl]pyrazine-2-carboxamide ($\mathrm{H}\mathbf{L^{1E}}$) were prepared in two or three steps from commercially available pyrazine-2-carboxylic acid (**1**) as shown in Scheme 1. Conversion of **1** to the methyl ester **2**·HCl was achieved by esterification with methanol and thionyl chloride, and the free base **2** obtained from that by treatment with potassium carbonate.

The addition of either 2 equiv. of 2-(2-aminoethyl)pyridine to **2**·HCl, or of 1 equiv. of 2-(2-aminoethyl)pyridine to **2** in methanol resulted in the formation of the desired new ligand $\mathrm{H}\mathbf{L^{1E}}$. Silica gel column chromatography allowed the purification of the ligand, affording $\mathbf{HL^{1E}}$ in quantitative or 39% yield, respectively. Surprisingly, the synthesis of $\mathrm{H}\mathbf{L^{1E}}$ from the free base **2** resulted in a lower yield: not all of the ester reacted but no amine was left. A repeat of this experiment with a slight excess of amine should improve the yield considerably. However, as the use of **2**·HCl worked well this was not pursued.

The methylene analogue $\mathrm{H}\mathbf{L^{1M}}$ was prepared from **2** and 1 equiv. of 2-(2-aminoethyl)pyridine. After column chromatography, the product was further purified by vapour diffusion of diethyl ether into a dichloromethane solution to give colourless rod-like crystals of $\mathrm{H}\mathbf{L^{1M}}$ in 75% yield.

Mononuclear "Building Block" Cobalt(III) Complexes

Both cobalt complexes were prepared in air in acetonitrile by treating 2 equiv. of the ligand with 2 equiv. of triethylamine before adding 1 equiv. of cobalt(II) tetrafluoroborate hexahydrate. Slow diffusion of diethyl ether vapour into the acetonitrile solutions gave the products as deep-red single crystals. Decanting of the solvent and drying of the residue in vacuo gave $[\mathrm{Co^{III}}(\mathbf{L^{1E}})_2](\mathrm{BF_4})\cdot\tfrac{1}{2}\mathrm{H_2O}$ and $[\mathrm{Co^{III}}(\mathbf{L^{1M}})_2](\mathrm{BF_4})\cdot\tfrac{1}{4}\mathrm{H_2O}$ in 83% and 32% yields, respectively. Consistent with air oxidation to diamagnetic $\mathrm{Co^{III}}$, sharp ^{1}H and ^{13}C NMR spectra were obtained and assigned for each complex.

Mass spectrometric data obtained on an "aged" sample of $[\mathrm{Co^{III}}(\mathbf{L^{1M}})_2](\mathrm{BF_4})\cdot\tfrac{1}{4}\mathrm{H_2O}$, that had been stirred in solution for 3 d in air before being crystallised, revealed signals consistent with the presence of both $[\mathrm{Co^{III}}(\mathbf{L^{1M}})(\mathbf{L^{1Mox}})]^+$ and $[\mathrm{Co^{III}}(\mathbf{L^{1Mox}})_2]^+$ species (Figure 3). There is precedent for oxidation of the methylene linker, Mascharak and coworkers having reported that this occurred for the cobalt complex of the analogous pyridyl ligand $(\mathbf{L^7})^-$, forming $(\mathbf{L^{7ox}})^-$ (Figure 2).[14] In order to isolate a pure sample of the non-oxidised ligand product, $[\mathrm{Co^{III}}(\mathbf{L^{1M}})_2](\mathrm{BF_4})$, the synthesis was repeated and the solid material isolated by overnight crystallisation within 12 h. Electrochemical experiments on $[\mathrm{Co^{III}}(\mathbf{L^{1M}})_2](\mathrm{BF_4})$ showed that this complex was stable in the solid state in air for at least two weeks.

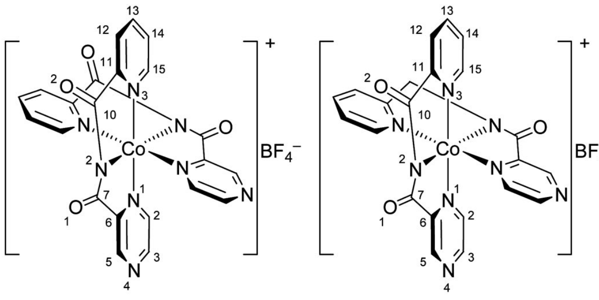

Figure 3. In the case of the methylene-linked ligand, ligand oxidation appears to lead to the formation of $[\mathrm{Co^{III}}(\mathbf{L^{1M}})(\mathbf{L^{1Mox}})](\mathrm{BF_4})$ (right) and $[\mathrm{Co^{III}}(\mathbf{L^{1Mox}})_2](\mathrm{BF_4})$ (left).

Single-crystal X-ray analyses (Figures 4 and 5) confirmed that in both cases the cobalt(II) ion had been air-oxidised to cobalt(III). Two mono-deprotonated $(\mathbf{L^{1E}})^-$ or $(\mathbf{L^{1M}})^-$ ligands and one $\mathrm{BF_4}$ anion are present per cobalt centre, implying a +III oxidation state. Consistent with this, the Co–N bond lengths are appropriate for low-spin cobalt(III) {1.91–1.99 Å for $[\mathrm{Co^{III}}(\mathbf{L^{1E}})_2](\mathrm{BF_4})\cdot 2\mathrm{CH_3CN}$ and 1.873–1.946 Å for $[\mathrm{Co^{III}}(\mathbf{L^{1M}})_2](\mathrm{BF_4})\cdot\tfrac{1}{4}\mathrm{H_2O}$}.

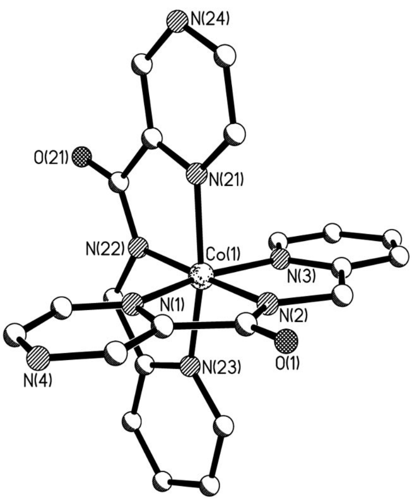

Figure 4. Perspective view of the cation of $[\mathrm{Co^{III}}(\mathbf{L^{1M}})_2](\mathrm{BF_4})\cdot\tfrac{1}{4}\mathrm{H_2O}$. Hydrogen atoms and anions omitted for clarity.

Each of the terdentate ligands is bound in a *mer* configuration through a pyridine, a deprotonated amide and a pyrazine nitrogen atom, forming an $\mathrm{N_6}$ octahedral geometry around the cobalt(III) ion. The two outward pointing "spare" pyrazine nitrogen donors per complex are approximately orthogonal to one another.

Within these complexes, each of the methylene-linked ligands was found to be very flat [pyridine and pyrazine rings almost coplanar N(1)/N(3) 4.6(2)° and N(21)/N(23) 0.6(1)°], whereas each of the ethylene-linked ligands was

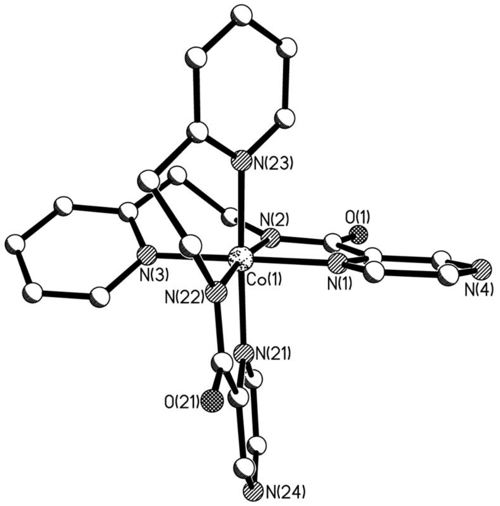

Figure 5. Perspective view of the cation of $[Co^{III}(\mathbf{L^{1E}})_2](BF_4)\cdot 2CH_3CN$. Hydrogen atoms and anions omitted for clarity.

found to be far more twisted [N(1)/N(3) 42.0(1)° and N(21)/N(23) 40.5(1)°]. The twisting of the latter ligands is facilitated by the conformationally more flexible ethylene linker; the methylene linker provides less flexibility.

Dimeric and Polymeric Silver(I) Complexes

The 1:1 reaction of silver(I) tetrafluoroborate with the appropriate ligand in acetonitrile in the dark followed by the slow diffusion of diethyl ether vapour into the acetonitrile solutions gave $[Ag^I_2(H\mathbf{L^{1E}})_2](BF_4)_2$ and $\{[Ag^I(H\mathbf{L^{1M}})](BF_4)\}_\infty$ as colourless block-shaped crystals in 68% and 50% yields, respectively. When triethylamine was used in attempts to deprotonate the amide group in the ligand, oily, unidentified products were obtained.

Single-crystal X-ray analyses (Figures 6 and 7) of these two silver complexes confirmed that the amide nitrogen atoms of the $H\mathbf{L^{1E}}$ and $H\mathbf{L^{1M}}$ ligands are not deprotonated. Rather, they remain neutral, and a tetrafluoroborate anion balances the charge of the silver(I) ion. In both cases, the asymmetric unit comprises one silver ion, one neutral ligand and a tetrafluoroborate counterion. The silver(I) atoms are bound to a pyrazine nitrogen atom of one ligand and a pyridine nitrogen atom (and weakly to an amide oxygen atom) of another ligand. In the case of the ethylene-linked ligand a dimeric structure results (second half of the dimer generated by a centre of inversion), whereas for the methylene-linked ligand a polymer results (Figures 6 and 7). The polymer consists of two intertwined helical strands running parallel to one another and interacting through Ag···Ag [3.3237(5) Å] and π–π interactions [centroid···centroid 3.704 Å; mean plane···centroid and offset angles: 3.441(1) Å and 21.7°; and 3.553(1) Å and 16.4°; mean planes intersect 11.3(2)°].

Considering only the nitrogen donor atoms, the silver(I) atoms in $\{[Ag^I(H\mathbf{L^{1M}})](BF_4)_2\}_\infty$ have an almost ideal linear geometry [N4–Ag1–N3B 176.4(1)°], whereas in $[Ag^I_2(H\mathbf{L^{1LE}})_2](BF_4)_2$ there is a significant distortion away from linear [N4–Ag1–N3A 158.6(1)°]. Consistent with this, the weak Ag–O bonds are shorter in the dimer than in the polymer [2.542(2) vs. 2.615(2) Å] and the Ag–N bonds slightly longer [2.179(2) and 2.167(2) Å vs. 2.153(3) and 2.158(3) Å].

Silver(I)-Connected Cobalt(III) Building Blocks

Initially, the reaction of the inert cobalt(III) building block, $[Co^{III}(\mathbf{L^{1E}})_2](BF_4)\cdot½H_2O$ with silver(I) nitrate in acetonitrile was carried out in a 1:1 ratio in an attempt to form a polymeric array of silver(I)-connected (through the "spare" pyrazine nitrogen donors) cobalt(III) complexes. Diethyl ether vapour diffusion into the resulting brown-red solution gave brown-red block-like single crystals. Elemental analysis, and the subsequent X-ray crystal structure determination (Figure 8) were consistent with this being a 2:1 Co^{III}/Ag^I complex, $\{[Co^{III}(\mathbf{L^{1E}})_2]_2[Ag^I(H_2O)]\}(BF_4)(NO_3)_2$ (no H_2O was present in the dried microanalysis sample), despite the 1:1 reaction stoichiometry. The yield, on the basis of the limiting reagent (the cobalt building block complex) was 94%. When the correct, 2:1 Co/Ag, reaction stoichiometry was employed the product obtained contained a 2:1 BF_4/NO_3 ratio, consistent with the ratio present in the reaction, not a 1:2 ratio as obtained from the 1:1 reaction.

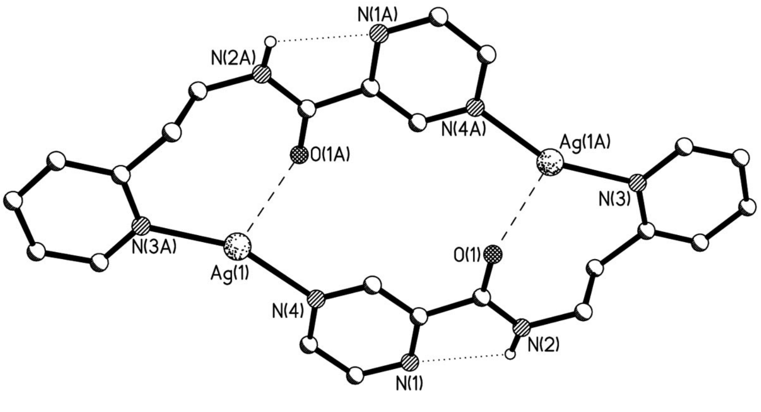

Figure 6. Perspective view of the cation of $[Ag^I_2(H\mathbf{L^{1E}})_2](BF_4)_2$. Hydrogen atoms, other than those on the amide nitrogen atoms, and anions omitted for clarity. A: –*x*, –*y*, –*z*.

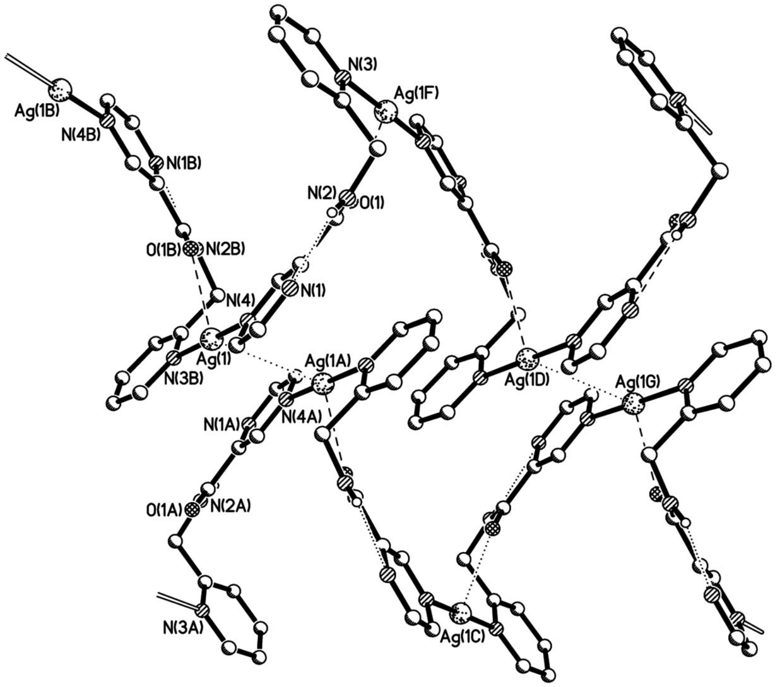

Figure 7. Perspective view of the cation of $\{[Ag^I(HL^{1M})](BF_4)\}_\infty$. Hydrogen atoms, other than those on the amide nitrogen atoms, and anions omitted for clarity. Two intertwined helical strands run left-right. A: 1 – *x*, –*y*, 2 – *z*; B: 1 – *x*, –0.5 + *y*, 1.5 – *x*.

No single crystals were obtained from the 2:1 reaction. A product with a 1:1 Co/Ag ratio was not obtained, even when an excess (10×) of silver(I) was used.

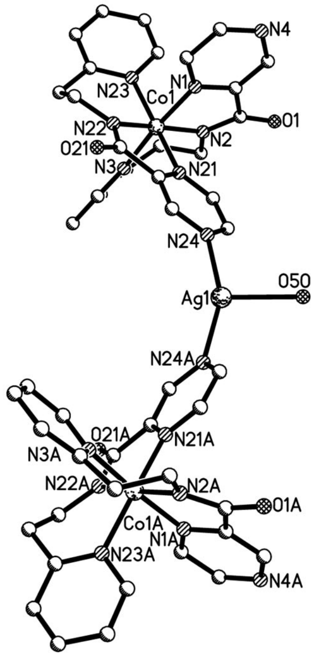

Figure 8. Perspective view of the cation of $\{[Co^{III}(L^{1E})_2]_2[Ag^I(H_2O)]\}(BF_4)(NO_3)_2$. Hydrogen atoms and anions omitted for clarity. A: 1 – *x*, *y*, 0.5 – *z*.

The single-crystal X-ray structure confirmed that, as desired, the silver(I) ion (located on a C_2 axis) has bridged two crystallographically identical cobalt(III) sub-units by one of their "spare" pyrazine donor atoms [Figure 8; Ag1–N24 2.209(3) Å, N24–Ag1–N24A 155.4(1)°] forming the 2:1 dimer $\{[Co^{III}(L^{1E})_2]_2[Ag^I(H_2O)]\}(BF_4)(NO_3)_2$. The silver(I) atom is also weakly bound to the oxygen atom of a water molecule of crystallisation [Ag1···O50 2.414(4) Å] causing the N–Ag–N angle [155.4(1)°] to be distorted somewhat away from linear. The silver(I) atom also has a very weak interaction with the nitrate anion [Ag–O 2.780(3) Å]. As expected, the Co–N distances are within experimental error of those observed for the mono-cobalt(III) complex $[Co^{III}(L^{1E})_2](BF_4)\cdot 2CH_3CN$, despite the intra-ligand pyrazine ring to pyridine ring angles [36.0(1)° and 48.2(1)°] being more widely spread than for $[Co^{III}(L^{1E})_2](BF_4)\cdot 2CH_3CN$ [40.5(1)° and 42.0(1)°].

Electrochemical Studies

Electrochemical analysis of $[Co^{III}(L^{1E})_2](BF_4)\cdot ½H_2O$ over a wide range (–2.0 to +2.0 V) showed the presence of a single chemically reversible reductive process (Figure 9, top). Close inspection of this process (Figure S3) showed it to have an $E_{1/2}$ of –0.48 V (ΔE = 75, 80, 90 and 95 mV, for scan rates of 50, 100, 200 and 400 mV s^{-1}, respectively). A controlled potential coulometry experiment at –0.59 V resulted in a change in colour from dark-red to pale-tan and the transfer of 0.96 electron-equiv., confirming that this is a one-electron reduction process, presumably primarily metal-centred ($Co^{III} \rightarrow Co^{II}$). Afterwards, the cyclic voltammogram was practically unchanged, consistent with chemical reversibility.

In contrast, an initial electrochemical analysis of the methylene-linked analogue, carried out on a solution-aged

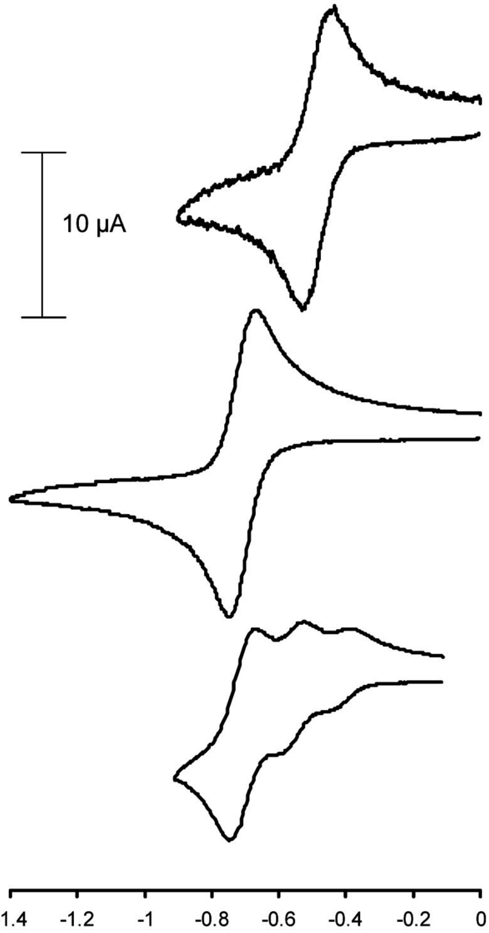

Figure 9. Cyclic voltammograms of $[\mathrm{Co^{III}}(\mathbf{L^{1E}})_2](\mathrm{BF_4})\cdot\frac{1}{2}\mathrm{H_2O}$ (top), *fresh* $[\mathrm{Co^{III}}(\mathbf{L^{1M}})_2](\mathrm{BF_4})\cdot\frac{1}{4}\mathrm{H_2O}$ (middle), and *aged* $[\mathrm{Co^{III}}(\mathbf{L^{1M}})_2](\mathrm{BF_4})$ (bottom) that is believed to contain $[\mathrm{Co^{III}}(\mathbf{L^{1M}})(\mathbf{L^{1Mox}})](\mathrm{BF_4})$ and $[\mathrm{Co^{III}}(\mathbf{L^{1Mox}})_2](\mathrm{BF_4})$. 200 mV s^{-1}, vs. 0.01 M $\mathrm{AgNO_3/Ag}$.

sample, showed the presence of three reductive processes between –2.0 and +2.0 V. Close inspection of these processes (Figure 9, bottom) over a smaller potential range (–0.9 to –0.1 V) showed they had $E_{1/2}$ values of –0.71, –0.54 and –0.41 V at scan rates of 50, 100, 200 and 400 mV s^{-1} (ΔE values at 50 mV s^{-1} were 60, 60 and 50 mV respectively, and at 400 mV s^{-1} were 70, 70 and 60 mV). These three processes are believed to be due to the presence of three different compounds in solution, $[\mathrm{Co^{III}}(\mathbf{L^{1M}})_2](\mathrm{BF_4})$, $[\mathrm{Co^{III}}(\mathbf{L^{1M}})(\mathbf{L^{1Mox}})](\mathrm{BF_4})$, and $[\mathrm{Co^{III}}(\mathbf{L^{1Mox}})_2](\mathrm{BF_4})$, which arise due to partial ligand oxidation (Figure 3).

Only one chemically reversible process is observed (Figure 9, middle) when a fresh sample of $[\mathrm{Co^{III}}(\mathbf{L^{1M}})_2](\mathrm{BF_4})$ is studied between –2 and +2 V. Close inspection of this process (Figure S4) over a smaller potential range (–1.4 to 0 V) showed that it has an $E_{1/2}$ of –0.71 V (ΔE = 65, 70, 75, 80 mV) at scan rates of 50, 100, 200 and 400 mV s^{-1}. A small bump on the re-oxidation side of the wave indicated the presence of a trace of ligand-oxidised product in the mixture. Controlled potential coulometry conducted at –0.81 V indicated that 0.84 electron-equiv. were transferred. This, along with the ΔE values and similarities to the $[\mathrm{Co^{III}}(\mathbf{L^{1E}})_2](\mathrm{BF_4})\cdot\frac{1}{2}\mathrm{H_2O}$ complex (including the same colour change from dark-red to tan during the controlled potential electrolysis) indicates that this too is a one-electron process.

Tests of the hypothesis that the presence of three electrochemical processes in the experiment carried out on the “aged” sample was due to the presence of oxidised versions of the monomeric complex (Figure 3) were carried out. Firstly, air was bubbled through an acetonitrile solution of fresh complex for 2 h. The cyclic voltammogram was unchanged, indicating that such oxidation may occur quite slowly. Therefore, in a second test, a “fresh” sample was stirred in acetonitrile solution in air for 2 d. The resulting cyclic voltammogram showed a large peak at –0.41 V along with shoulders at –0.71 and –0.54 V. These peaks occur in similar positions to those for the “aged” sample, so it appears that the proposed oxidation does require considerable time; this is also consistent with our ability to grow crystals of unoxidised ligand complex overnight (Figure 4).

As anticipated, the reduction potentials confirm that the methylene-linked ligand (–0.71 V) is better able to stabilise cobalt(III) over cobalt(II) than the ethylene-linked ligand can (–0.48 V). Interestingly, both of these amide ligands are better at this than the rather rigid imide ligand, $(\mathbf{L^{7ox}})^-$ (see Introduction, $E_{1/2}$ approx. –0.22 V).[13]

Conclusions

Two carefully designed *pyrazine*-amide-linker-pyridine ligands, $\mathbf{HL^{1M}}$ and $\mathbf{HL^{1E}}$, that contain a spare nitrogen atom out the back, have been prepared. The silver(I) complexes of these ligands were found to be dimeric and polymeric, $[\mathrm{Ag^I_2}(\mathbf{HL^{1E}})_2](\mathrm{BF_4})_2$ and $\{[\mathrm{Ag^I}(\mathbf{HL^{1M}})](\mathrm{BF_4})\}_\infty$, respectively. One-off attempts to deprotonate and coordinate the monoanionic ligands to silver(I) were unsuccessful.

Two cobalt(III) building blocks, $[\mathrm{Co^{III}}(\mathbf{L^{1M}})_2](\mathrm{BF_4})\cdot\frac{1}{4}\mathrm{H_2O}$ and $[\mathrm{Co^{III}}(\mathbf{L^{1E}})_2](\mathrm{BF_4})\cdot\frac{1}{2}\mathrm{H_2O}$, were prepared and fully characterised. In solution, the methylene-linked ligand in the former complex appears to be sensitive to oxidation, generating complexes of the more conjugated ligand, $[\mathrm{Co^{III}}(\mathbf{L^{1M}})(\mathbf{L^{1Mox}})](\mathrm{BF_4})$ and $[\mathrm{Co^{III}}(\mathbf{L^{1Mox}})_2](\mathrm{BF_4})$. Cyclic voltammetry was found to be a sensitive tool for monitoring this proposed ligand oxidation. The electrochemical studies also confirmed the expectation that the complex of the ethylene-linked ligand is (a) resistant to such ligand oxidation and (b) more readily reduced than the complex of the methylene-linked ligand.

Silver(I) was successfully employed to connect two $[\mathrm{Co^{III}}(\mathbf{L^{1E}})_2](\mathrm{BF_4})\cdot\frac{1}{2}\mathrm{H_2O}$ building blocks, by coordination to a spare nitrogen atom from each building block, despite the cobalt(III) withdrawing electron density from the pyrazine ring. With this test result in hand, our focus is now firmly on targeting the self-assembly of extended two-dimensional paramagnetic polymetallic systems. These are likely to be easier to link as (a) the metal ions will be in +2, not +3, oxidation states and (b) there are eight spare pyrazine nitrogen atoms per [2×2] grid complex, and they will be better aligned with regard to packing of the resulting super complex in space, so many complementary links should be possible. Only a handful of such systems have been studied, all by Lehn and co-workers, which is an indication of the challenges inherent in such research. However, the results of this pilot study pave the way for our next generation of experiments, on the basis of previous work from our research group, but which nevertheless involve overcoming significant synthetic challenges.[7]

Experimental Section

General: Acetonitrile used was HPLC grade. Pyrazine-2-carboxylic acid, cobalt(II) tetrafluoroborate hexahydrate, silver(I) tetrafluoroborate and silver(I) nitrate were used as supplied. The 10% (v/v) triethylamine stock solution was prepared from 9 mL of acetonitrile (HPLC grade, dried with calcium hydride) and 1 mL of triethylamine (distilled from calcium hydride). ^{1}H and ^{13}C NMR spectra were recorded at 25 °C with a Varian 300 or 500 MHz Inova spectrometer. NMR assignments were determined by a combination of results from HSQC, gHMBC, gCOSY, ^{1}H and ^{13}C NMR spectra. ESI mass spectra were recorded in acetonitrile with a Bruker MicrOTOF$_Q$ spectrometer. All electrochemical analyses were conducted under argon with a 1 mmol L^{-1} solution of complex in dry acetonitrile with 0.1 mol L^{-1} $Bu_4N(PF_6)$ (recrystallised from water and dried in vacuo) electrolyte. All potentials are quoted vs. 0.01 mol L^{-1} $AgNO_3$/Ag. All controlled potential coulometry experiments were carried out until the current reached 1% of the initial value. The Fc/Fc$^+$ couple occurs at 0.07 V (75 mV) in this system. Single crystal X-ray data were collected with a Bruker SMART CCD area detector diffractometer (λ = 0.71073 Å). The structures were solved by direct methods using SHELXS-97[18] and refined against F^2 using full-matrix least-squares techniques with SHELXL-97.[18] A summary of the crystallographic data and refinement parameters is given in Table 1. CCDC-702959, -702960, -702961, -702962, -702963 contain the supplementary crystallographic data for this paper. These data can be obtained free of charge from The Cambridge Crystallographic Data Centre via www.ccdc.cam.ac.uk/data_request/cif.

Synthesis

2·HCl: Thionyl chloride (880 µL, 12.1 mmol) was added dropwise to a suspension of pyrazine-2-carboxylic acid (2.00 g, 16.1 mmol) in methanol (200 mL). The white solid rapidly dissolved and evolved a gas, leaving a clear colourless solution. After stirring for 2.5 d, the solution was concentrated to dryness in vacuo to give **2**·HCl as a white solid in quantitative yield. $C_6H_6N_2O_2$·HCl (174.59): calcd. C 41.28, H 4.04, N 16.05; found C 41.19, H 3.87, N 15.76.

2: Methyl pyrazine-2-carboxylate hydrochloride (**2**·HCl) (10.0 g, 57.3 mmol) was suspended in dichloromethane (200 mL). Potassium carbonate (10 g) was added and the mixture stirred for 1 h. The solution was decanted, filtered (glass sinter), and the solvents were evaporated to dryness in vacuo to yield 7.02 g (50.9 mmol, 89%) of **2** as a white solid. ^{1}H NMR (300 MHz, $CDCl_3$): δ = 9.33 (d, J = 1.5 Hz, 1 H, 5-H), 8.78 (d, J = 2.7 Hz, 1 H, 2-H), 8.73 (dd, $J_{3,5}$ = 1.5, $J_{3,2}$ = 2.4 Hz, 1 H, 3-H), 4.05 (s, 3 H, 9-H) ppm. $C_6H_6N_2O_2$ (138.13): calcd. C 52.17, H 4.38, N 20.28; found C 52.42, H 4.44, N 20.36.

HL^{1E}. Method A: A solution of methyl pyrazine-2-carboxylate hydrochloride (120 mg, 870 µmol) and excess 2-(2-aminoethyl)pyridine (208 µL, 1.74 mmol) in methanol (5 mL) was refluxed for 8 h and stirred at room temperature for 14 h, then concentrated to dryness in vacuo to give **HL^{1E}** as an off-white crystalline solid. The product was purified by column chromatography (silica gel, 5% MeOH/CH_2Cl_2, R_f = 0.25). The resulting yellow oil rapidly crystallised on cooling from 30 °C (rotary evaporator temperature) to 20 °C to give a pale lemon-coloured solid in quantitative yield. **Method B:** A solution of methyl pyrazine-2-carboxylate (**2**) (1.00 g, 7.25 mmol) and 2-(2-aminoethyl)pyridine (510 µL, 7.25 mmol) in methanol (40 mL) was refluxed for 4 d, then concentrated to dryness in vacuo to give **HL^{1E}** as an impure tan solid. The product was purified by column chromatography (silica gel, 5% MeOH/CH_2Cl_2, R_f = 0.25) to afford **HL^{1E}** as a white solid in 645 mg (2.83 mmol, 39%) yield. ^{1}H NMR (300 MHz, $CDCl_3$): δ = 9.35 (d, J = 1.5 Hz, 1 H, 5-H), 8.67 (d, J = 2.4 Hz, 1 H, 3-H), 8.54 (d, J = 7.5 Hz, 1 H, 16-H), 8.47 (dd, $J_{2,5}$ = 1.5, J = 2.4 Hz, 1 H, 2-H), 8.45 (br. s, 1 H, NH), 7.58 (dt, J = 7.5, J = 1.5 Hz, 1 H, 15-H), 7.15 (m, 2 H, 13-H and 14-H), 3.88 (q, J = 6.6 Hz, 2 H, 10-H), 3.09 (t, J = 6.3 Hz, 2 H, 11-H) ppm. ^{13}C NMR (300 MHz, $CDCl_3$): δ = 163.0 (C-7), 159.0 (C-12), 149.3 (C-16), 147.0 (C-3), 144.7 (C-6), 144.3 (C-5), 142.6 (C-2), 136.7 (C-15), 123.4 (C-13), 121.6 (C-14), 38.7 (C-10) and 37.1 (C-11) ppm. $C_{12}H_{12}N_4O$ (228.25): calcd. C 63.15, H 5.30, N 24.55; found C 63.23, H 5.52, N 24.54.

HL^{1M}: A solution of methyl pyrazine-2-carboxylate (**2**) (2.00 g, 14.5 mmol) and 2-(aminomethyl)pyridine (1.50 mL, 14.5 mmol) in methanol (80 mL) was refluxed for 5 d, before concentrating to dryness in vacuo, to yield **HL^{1M}** as a tan solid. The product was purified by column chromatography (silica gel, 5% MeOH/CH_2Cl_2, R_f = 0.25) to afford **HL^{1M}** as an off-white solid. Diffusion of diethyl ether into a solution of the product in dichloromethane yielded 2.25 g (10.5 mmol, 73%) of white rod-like crystals of **HL^{1M}**. ^{1}H NMR (500 MHz, $CDCl_3$): δ = 9.42 (s, 1 H, 5-H), 8.86 (br. s, 1 H, 9-H), 8.75 (d, J = 2.5 Hz, 1 H, 3-H), 8.610 (td, J = 5, J = 1.2 Hz, 1 H, 15-H), 8.57 (d, J = 2.5 Hz, 2 H, 2-H), 7.70 (dt, J = 8.0, J = 1.2 Hz, 1 H, 13-H), 7.36 (d, J = 7.5 Hz, 1 H, 12-H), 7.24 (t, J = 5 Hz, 1 H, 14-H) and 4.81 (d, J = 7.5 Hz, 1 H, 10-H) ppm. ^{13}C NMR (500 MHz, $CDCl_3$): δ = 166.2 (C-7), 156.1 (C-6), 149.1 (C-15), 147.3 (C-3), 144.6 (C-11), 144.5 (C-5), 142.8 (C-2), 137.2 (C-13), 122.7 (C-14), 122.3 (C-12) and 44.4 (C-10) ppm. $C_{11}H_{10}N_4O$ (214.23): calcd. C 61.67, H 4.71, N 26.15; found C 61.71, H 4.58, N 26.37.

[Co^{III}(L^{1E})$_2$](BF$_4$)·½H$_2$O: Triethylamine (49 µL, 351 µmol) was added to a solution of **HL^{1E}** (80.0 mg, 351 µmol) in acetonitrile (7 mL) and stirred for 30 min, before cobalt(II) tetrafluoroborate hexahydrate (60.0 mg, 176 µmol) was added. The resulting orange-red solution was stirred overnight. The solution was then reduced in volume in vacuo to ca. 5 mL. Slow diffusion of diethyl ether vapour into this solution resulted in deep-red, very large (up to 3 mm across), plate-shaped single crystals of [Co^{III}(**L^{1E}**)$_2$](BF$_4$)·2CH$_3$CN. The colourless solution was decanted, and the crystals dried in vacuo to give 88.8 mg (148 µmol, 83%) of [Co^{III}(**L^{1E}**)$_2$](BF$_4$)·½H$_2$O. ^{1}H NMR (500 MHz, CD_3CN): δ = 9.08 (s, 1 H, 5-H), 8.53 (d, J = 3 Hz, 1 H, 3-H), 8.26 (d, J = 6 Hz, 1 H, 16-H), 8.01 (d, J = 3 Hz, 1 H, 2-H), 7.818 (t, J = 8 Hz, 1 H, 14-H), 7.36 (d, J = 7.5 Hz, 1 H, 13-H), 7.24 (t, J = 7 Hz, 1 H, 15-H), 4.67 (td, J = 4, J = 14 Hz, 1 H, 10-H), 3.65 (dt, J = 14, J = 2 Hz, 1 H, 11-H), 3.21 (m, 1 H, 10-H), 2.37 (dt, J = 18, J = 4 Hz, 1 H, 11-H) ppm. ^{13}C NMR (500 MHz, CD_3CN): δ = 171.2 (C-7), 165.6 (C-6), 154.7 (C-16), 150.6 (C-12), 150.2 (C-3), 147.6 (C-5), 146.5 (C-2), 142.0 (C-14), 129.1 (C-13), 125.4 (C-15), 41.6 (C-10), 37.8 (C-11) ppm. MS (ESI): m/z = 513 [Co^{III}(**L^{1E}**)$_2$]$^+$. $C_{24}H_{22}BCoF_4N_8O_2$·½H$_2$O (609.24): calcd. C 47.32, H 3.81, N 18.39; found C 47.40, H 3.79, N 18.53.

Table 1. Details of the crystal-structure determination for the complexes $[Co^{III}(\mathbf{L^{1E}})_2](BF_4)\cdot 2CH_3CN$, $[Co^{III}(\mathbf{L^{1M}})_2](BF_4)\cdot \tfrac{1}{4}H_2O$, $[Ag^{I}(H\mathbf{L^{1LE}})]_2(BF_4)_2$, $\{[Ag^{I}(H\mathbf{L^{1M}})]BF_4\}_\infty$ and $[\{Co^{III}(\mathbf{L^{1E}})_2\}_2Ag^{I}(OH_2)](BF_4)(NO_3)_2$.

	$[Co^{III}(\mathbf{L^{1E}})_2](BF_4)\cdot 2CH_3CN$	$[Co^{III}(\mathbf{L^{1M}})_2]\cdot(BF_4)\cdot \tfrac{1}{4}H_2O$	$[Ag^{I}_2(H\mathbf{L^{1E}})_2]\cdot(BF_4)_2$
Empirical formula	$C_{28}H_{28}BCoF_4N_{10}O_2$	$C_{22}H_{18.50}BCoF_4N_8O_{2.25}$	$C_{24}H_{24}Ag_2B_2F_8N_8O_2$
M_r	682.34	576.69	845.87
Crystal system	triclinic	monoclinic	triclinic
Space group	$P\bar{1}$	$P2_1/c$	$P\bar{1}$
a [Å]	8.8824(5)	9.9828(13)	8.0720(5)
b [Å]	10.1800(6)	8.4576(8)	8.9336(5)
c [Å]	15.9646(10)	27.226(3)	10.3831(6)
α [°]	93.602(3)	90	102.802(3)
β [°]	91.676(3)	92.193(4)	103.376(2)
γ [°]	94.560(3)	90	90.646(3)
V [Å^3]	1435.30(15)	2297.0(5)	708.78(7)
Z	2	4	1
$\rho_{calcd.}$ [g/cm^3]	1.579	1.668	1.982
μ [mm]$^{-1}$	0.672	0.821	1.475
$F(000)$	700	1170	416
Crystal size [mm]	0.45 × 0.30 × 0.14	0.45 × 0.20 × 0.15	0.54 × 0.14 × 0.04
θ range for data collection [°]	2.01–26.53	1.50–26.52	2.07–26.00
Reflections collected	30408	29029	14517
Independent reflections	5933	4762	2720
R(int)	0.0280	0.0533	0.0338
Max./min. transmission	1.000/0.911	0.887/0.709	0.943/0.503
Data/restraints/parameters	5933/16/439	4762/9/363	2720/1/212
Goof (F^2)	1.042	1.033	1.058
R_1 [$I > 2\sigma(I)$]	0.0280	0.0476	0.0210
wR_2 (all data)	0.0701	0.1238	0.0526

	$\{[Ag^{I}(H\mathbf{L^{1M}})]\cdot BF_4\}_\infty$	$[\{Co^{III}(\mathbf{L^{1E}})_2\}_2Ag^{I}(OH_2)](BF_4)(NO_3)_2$
Empirical formula	$C_{11}H_{10}AgBF_4N_4O$	$C_{48}H_{46}AgBCo_2F_4N_{18}O_{11}$
M_r	408.91	1363.57
Crystal system	monoclinic	monoclinic
Space group	$P2_1/c$	$P2/c$
a [Å]	10.0079(6)	19.3281(14)
b [Å]	8.4784(5)	12.7845(9)
c [Å]	15.6539(10)	10.3147(7)
α [°]	90	90
β [°]	99.002(3)	90.949(4)
γ [°]	90	90
V [Å^3]	1311.89(14)	2548.4(3)
Z	4	2
$\rho_{calcd.}$ [g/cm^3]	2.070	1.777
μ [mm]$^{-1}$	1.590	1.121
$F(000)$	800	1380
Crystal size [mm]	0.30 × 0.10 × 0.05	0.50 × 0.10 × 0.05
θ range for data collection [°]	2.74–26.40	2.11–26.02
Reflections collected	18644	64154
Independent reflections	2686	5023
R(int)	0.0521	0.0611
Max./min. transmission	0.924/0.647	1.000/0.837
Goof (F^2)	1.098	1.099
R_1 [$I > 2\sigma(I)$]	0.0347	0.0342
wR_2 (all data)	0.0877	0.0698

$[Co^{III}(\mathbf{L^{1M}})_2](BF_4)\cdot \tfrac{1}{4}H_2O$: $H\mathbf{L^{1M}}$ (40.0 mg, 187 µmol) and triethylamine [187 µmol, 261 µL of 10% (v/v) stock solution in acetonitrile] were stirred in acetonitrile (10 mL) for 30 min. Cobalt(II) tetrafluoroborate hexahydrate (31.8 mg, 93.5 µmol) in acetonitrile (1 mL) was added with stirring, resulting in a dark red solution, which was stirred overnight. Diffusion of diethyl ether vapour into the solution over 7 d gave a red solid in a colourless solution. The colourless solution was decanted and discarded. The red solid was redissolved in acetonitrile. Diffusion of diethyl ether vapour into the solution gave red rod-like crystals surrounded by red powder in a red solution. The solvent was decanted and the solids dried in vacuo to give 34.8 mg (60.4 µmol, 32%) of $[Co^{III}(\mathbf{L^{1M}})_2](BF_4)\cdot \tfrac{1}{4}H_2O$. ^{1}H NMR (500 MHz, CD_3NO_2): δ = 9.05 (d, J = 1.0 Hz, 1 H, 5-H), 8.58 (d, J = 3.0 Hz, 1 H, 3-H), 8.25 (d, J = 2.5, J = 1.2 Hz, 1 H, 2-H), 8.18 (dd, J = 7.5, J = 1.2 Hz, 1 H, 15-H), 7.87 (dt, J = 8, J = 1.2 Hz, 1 H, 13-H), 7.67 (dd, J = 8, J = 1.5 Hz, 1 H, 12-H), 7.29 (dt, J = 8, J = 1.5 Hz, 1 H, 14-H), 5.93 (s, 1 H, 10-H) and 5.90 (s, 1 H, 10-H) ppm. ^{13}C NMR (125 MHz, CD_3NO_2): δ = 52.2 (C-10), 125.3 (C-12), 127.0 (C-14), 141.8 (C-13), 146.9 (C-5), 147.0 (C-2), 150.9 (C-3), 151.7 (C-15), 152.3 (C-6), 168.9 (C-7), 169.0 (C-11) ppm. MS (ESI): m/z = 485 $[\mathrm{Co^{III}}(\mathbf{L^{1M}})_2]^+$, 499 $[\mathrm{Co^{III}}(\mathrm{O}\mathbf{L^{1M}})_2]^+$, 513 $[\mathrm{Co^{III}}(\mathrm{O}\mathbf{L^{1M}})(\mathrm{O}\mathbf{L^{1M}})]^+$. $C_{22}H_{18}BCoF_4N_8O_2 \cdot \frac{1}{4}H_2O$ (576.68): calcd. C 45.82, H 3.23, N 19.43; found C 45.51, H 3.20, N 19.43.

$[\mathrm{Ag^I}_2(\mathrm{H}\mathbf{L^{1E}})_2](\mathrm{BF_4})_2$: Silver(I) tetrafluoroborate (69.2 mg, 355 µmol) in acetonitrile (2 mL) was added to $\mathrm{H}\mathbf{L^{1E}}$ (81.0 mg, 355 µmol) in acetonitrile (7 mL) resulting in a lemon-coloured solution, which was stirred at room temperature for 4 h. Diffusion of diethyl ether vapour into the solution in the dark over 10 d gave 103 mg (79.1 µmol, 67%) of $[\mathrm{Ag^I}_2(\mathrm{H}\mathbf{L^{1E}})_2](\mathrm{BF_4})_2$ as microanalytically pure, clear, colourless, rod-shaped crystals. ^{1}H NMR (300 MHz, CD_3CN): δ = 10.17 (s, 1 H, 5-H), 8.95 (d, J = 2.5 Hz, 1 H, 3-H), 8.93 (d, J = 2.5 Hz, 1 H, 2-H), 8.76 (d, J = 7.5 Hz, 1 H, 16-H), 8.07 (t, J = 7.5 Hz, 1 H, 14-H), 7.69 (d, J = 7.5 Hz, 1 H, 13-H), 7.56 (t, J = 7.5 Hz, 1 H, 15-H), 3.88 (m, 2 H, 11-H), 3.40 (m, 1 H, 10-H) ppm. ^{13}C NMR (125 MHz, CD_3CN): δ = 165.5 (C-7), 160.4 (C-12), 153.5 (C-16), 149.8 (C-2), 147.4 (C-6), 146.8 (C-5), 146.6 (C-3), 141.6 (C-14), 126.9 (C-13), 124.8 (C-15), 41.8 (C-11), 41.5 (C-10) ppm. $C_{12}H_{11}AgBF_4N_4O$ (421.92): calcd. C 34.16, H 2.63, N 13.28; found C 34.23, H 2.93, N 13.14.

$\{[\mathrm{Ag^I}(\mathrm{H}\mathbf{L^{1M}})]\mathrm{BF_4}\}_\infty$: Silver(I) tetrafluoroborate (36.4 mg, 187 µmol) in acetonitrile (1 mL) was added to $\mathrm{H}\mathbf{L^{1M}}$ (40.0 mg, 187 µmol) in acetonitrile (5 mL) resulting in a colourless solution, which was stirred in the dark for 30 min. Diffusion of diethyl ether vapour into the solution in the dark over 3 d gave $\{[\mathrm{Ag^I}(\mathrm{H}\mathbf{L^{1M}})](\mathrm{BF_4})\}_\infty$ as microanalytically pure, clear, colourless, rod-shaped crystals in 38.2 mg (93.4 µmol, 50%) yield. ^{1}H NMR (300 MHz, CD_3CN): δ = 9.26 (d, $J_{2,5}$ = 1.5 Hz, 1 H, 5-H), 8.78 (d, J = 2.7 Hz, 1 H, 3-H), 8.75 (br. s, 1 H, 9-H), 8.62 (dd, J = 2.4, $J_{2,5}$ = 1.5 Hz, 1 H, 2-H), 8.53 (m, 1 H, 12-H), 7.81 (dt, J = 7.8, J = 2.1 Hz, 1 H, 13-H), 7.44 (d, J = 7.8 Hz, 1 H, 15-H), 7.33 (m, 1 H, 14-H), 4.73 (d, J = 6.0 Hz, 2 H, 10-H) ppm. ^{13}C NMR (125 MHz, CD_3CN): δ = 45.8 (C-10), 118.3 (C-7), 123.3 (C-15), 123.9 (C-14), 138.8 (C-13), 144.3 (C-2), 144.9 (C-5), 145.6 (C-6), 148.8 (C-3), 150.8 (C-12), 158.5 (C-11), 164.5 (C-7) ppm. $C_{11}H_{10}AgBF_4N_4O$ (408.90): calcd. C 32.31, H 2.47, N 13.70; found C 32.49, H 2.53, N 13.84.

$[\{\mathrm{Co^{III}}(\mathbf{L^{1E}})_2\}_2\mathrm{Ag^I}](\mathrm{BF_4})(\mathrm{NO_3})_2$: Silver(I) nitrate (8.1 mg, 47.7 µmol) was added to a solution of $[\mathrm{Co^{III}}(\mathbf{L^{1E}})_2](\mathrm{BF_4})\cdot\frac{1}{2}H_2O$ (29.2 mg, 47.9 µmol) in acetonitrile (4 mL). The resulting dark-red solution was stirred overnight. Slow diffusion of diethyl ether vapour into this solution resulted in deep-red plate-shaped single crystals of $[\{\mathrm{Co^{III}}(\mathbf{L^{1E}})_2\}_2\mathrm{Ag^I}(\mathrm{OH_2})](\mathrm{BF_4})(\mathrm{NO_3})_2$. The colourless solution was decanted and the crystals dried in vacuo to give 30.2 mg (22.5 µmol, 94% based on the limiting reagent, the cobalt complex) of $[\{\mathrm{Co^{III}}(\mathbf{L^{1E}})_2\}_2\mathrm{Ag^I}](\mathrm{BF_4})(\mathrm{NO_3})_2$. ^{1}H NMR (300 MHz, CD_3CN): δ = 9.07 (d, J = 3.3 Hz, 1 H, 5-H), 8.53 (t, ^3J = 3.3 Hz, 1 H, 2-H), 8.25 (m, 1 H, 16-H), 8.00 (t, J = 3.3 Hz, 1 H, 3-H), 7.81 (m, 1 H, 14-H), 7.34 (dd, J = 7.8, J = 1.8 Hz, 1 H, 13-H), 7.24 (m, 1 H, 15-H), 4.65 (m, 1 H, 10-H), 3.65 (t, J = 14, J = 3.6 Hz, 1 H, 10-H), 3.19 (dd, J = 14.0, J = 2.4 Hz, 1 H, 11-H), 2.35 (tt, J = 14.0, J = 3.6 Hz, 1 H, 11-H) ppm. ^{13}C NMR (125 MHz, CD_3NO_2): δ = 41.6 (C-10), 37.8 (C-11), 125.4 (C-15), 129.1 (C-13), 142.0 (C-14), 146.6 (C-6), 147.6 (C-5), 150.2 (C-3), 150.6 (C-2), 154.6 (C-16), 165.6 (C-12), 171.4 (C-7) ppm. $C_{48}H_{44}AgBCo_2F_4N_{18}O_{10}$ (1345.53): calcd. C 42.85, H 3.30, N 18.74; found C 43.14, H 3.32, N 18.46.

$[\{\mathrm{Co^{III}}(\mathbf{L^{1E}})_2\}_2\mathrm{Ag^I}](\mathrm{BF_4})_2(\mathrm{NO_3})$: Silver(I) nitrate (16.4 µmol, from 0.5 mL of 32.8 mmol L^{-1} stock solution in acetonitrile) was added to a solution of $[\mathrm{Co^{III}}(\mathbf{L^{1E}})_2](\mathrm{BF_4})\cdot\frac{1}{2}H_2O$ (20.0 mg, 32.8 µmol) in acetonitrile (5 mL). The resulting dark-red solution was stirred overnight. Slow diffusion of diethyl ether vapour into this solution resulted in a deep-red solid. The colourless solution was decanted, and the crystals were dried in vacuo to give 16.4 mg (12.0 µmol, 73%) of $[\{\mathrm{Co^{III}}(\mathbf{L^{1E}})_2\}_2\mathrm{Ag^I}](\mathrm{BF_4})_2(\mathrm{NO_3})$. $C_{48}H_{44}AgB_2Co_2F_8N_{16}NO_4O_3$ (1370.33): calcd. C 42.07, H 3.24, N 17.38; found C 41.94, H 3.69, N 17.28.

Supporting Information (see also the footnote on the first page of this article): Further crystallographic details and diagrams, as well as additional cyclic voltammetry plots (including scan-rate and full-range studies).

Acknowledgments

This work was supported by grants from the Marsden Fund (Royal Society of New Zealand) and the University of Otago. We thank Assoc. Prof. A. J. McQuillan for helpful discussions.

[1] a) M. Ruben, J. Rojo, F. J. Romero-Salguero, L. H. Uppadine, J.-M. Lehn, *Angew. Chem. Int. Ed.* **2004**, *43*, 3644; b) L. N. Dawe, T. S. M. Abedin, L. K. Thompson, *Dalton Trans.* **2008**, 1661.

[2] E. Breuning, M. Ruben, J.-M. Lehn, F. Renz, Y. Garcia, V. Ksenofontov, P. Gütlich, E. Wegelius, K. Rissanen, *Angew. Chem. Int. Ed.* **2000**, *39*, 2504.

[3] M. Ruben, E. Breuning, J. P. Gisselbrecht, J.-M. Lehn, *Angew. Chem. Int. Ed.* **2000**, *39*, 4139.

[4] a) E. B. Fleischer, M. B. Lawson, *Inorg. Chem.* **1972**, *11*, 2772; b) E. B. Fleischer, D. Jeter, R. Florian, *Inorg. Chem.* **1974**, *13*, 1042; c) I. Mallik, S. Mallik, *Synlett* **1996**, 734; d) D. S. Cati, H. Stoeckli-Evans, *Acta Crystallogr., Sect. E* **2004**, *60*, o210; e) D. S. Cati, H. Stoeckli-Evans, *Acta Crystallogr., Sect. E* **2004**, *60*, m174; f) D. S. Cati, H. Stoeckli-Evans, *Acta Crystallogr., Sect. E* **2004**, *60*, m177.

[5] a) J. Hausmann, G. B. Jameson, S. Brooker, *Chem. Commun.* **2003**, 2992; b) D. S. Cati, J. Ribas, J. Ribas-Arino, H. Stoeckli-Evans, *Inorg. Chem.* **2004**, *43*, 1021; c) J. Hausmann, S. Brooker, *Chem. Commun.* **2004**, 1530; d) J. Klingele (nee Hausmann), J. F. Boas, J. R. Pilbrow, B. Moubaraki, K. S. Murray, K. J. Berry, K. A. Hunter, G. B. Jameson, P. D. W. Boyd, S. Brooker, *Dalton Trans.* **2007**, 633.

[6] M. Ruben, U. Ziener, J.-M. Lehn, V. Ksenofontov, P. Guetlich, G. B. M. Vaughan, *Chem. Eur. J.* **2005**, *11*, 94.

[7] M. G. Cowan, D. S. Larsen, S. Brooker, unpublished results.

[8] *Scifinder Scholar 2007*, Chemical Abstracts Service, American Chemical Society, Columbus, Ohio, **2007**.

[9] a) J. I. Kim, H. S. Yoo, E. K. Koh, H. C. Kim, C. S. Hong, *Inorg. Chem.* **2007**, *46*, 8481; b) J. I. Kim, H. S. Yoo, E. K. Koh, C. S. Hong, *Inorg. Chem.* **2007**, *46*, 10461.

[10] D. L. Cockriel, J. M. McClain, K. C. Patel, R. Ullom, T. R. Hasley, S. J. Archibald, T. J. Hubin, *Inorg. Chem. Commun.* **2008**, *11*, 1.

[11] M. Nonoyama, K. Yamasaki, *Inorg. Chim. Acta* **1971**, *5*, 124.

[12] a) F. A. Chavez, C. V. Nguyen, M. M. Olmstead, P. K. Mascharak, *Inorg. Chem.* **1996**, *35*, 6282; b) T. Hirao, T. Moriuchi, T. Ishikawa, K. Nishimura, S. Mikami, Y. Ohshiro, I. Ikeda, *J. Mol. Catal. A* **1996**, *113*, 117; c) F. A. Chavez, J. M. Rowland, M. M. Olmstead, P. K. Mascharak, *J. Am. Chem. Soc.* **1998**, *120*, 9015; d) P. T. Kaye, T. Nyokong, G. M. Watkins, K. W. Wellington, *ARKIVOC* **2002**, *9*, 9; e) A. N. Dwyer, M. C. Grossel, P. N. Horton, *Supramol. Chem.* **2004**, *16*, 405; f) N. W. Alcock, G. Clarkson, P. B. Glover, G. A. Lawrance, P. Moore, M. Napitupulu, *Dalton Trans.* **2005**, 518; g) M. Napitupulu, G. A. Lawrance, G. J. Clarkson, P. Moore, *Aust. J. Chem.* **2006**, *59*, 796–804.

[13] T. Kajiwara, R. Sensui, T. Noguchi, A. Kamiyama, T. Ito, *Inorg. Chim. Acta* **2002**, *337*, 299.

[14] J. M. Rowland, M. M. Olmstead, P. K. Mascharak, *Inorg. Chem.* **2002**, *41*, 2754.

[15] A. Kamiyama, T. Noguchi, T. Kajiwara, T. Ito, *Inorg. Chem.* **2002**, *41*, 507.
[16] H. Chowdhury, S. H. Rahaman, R. Ghosh, S. K. Sarkar, H.-K. Fun, B. K. Ghosh, *J. Mol. Struct.* **2007**, *826*, 170.
[17] A. J. Bard, L. R. Faulkner, *Electrochemical methods: fundamentals and applications*, 2nd ed., John Wiley & Sons, Inc., New York, **2001**.
[18] G. M. Sheldrick, *Acta Crystallogr., Sect. A* **2008**, *64*, 112.

Received: December 7, 2008